ORIGINAL PAPER

Synthesis of carbon microtubules core structure LiFePO$_4$ via a template-assisted method

Turdi Wumair · Junqing Dou · Lu Zhang · Mingde Chen · Xueya Kang

Abstract The carbon microtubules core structure LiFePO$_4$ is synthesized using a cotton fiber template-assisted method. The crystalline structure and morphology of the product is characterized by X-ray diffraction and field emission scanning electron microscopy. The charge–discharge kinetics of the LiFePO$_4$ electrode is investigated using cyclic voltammetry and electrochemical impedance spectroscopy. The result shows that the well-crystallized carbon microtubules core structure LiFePO$_4$ is successfully synthesized. The as-synthesized material exhibits a high initial discharge capacity of 167 mAh g^{-1} at 0.2 C rate. The material also shows good high-rate discharge performance and cycling stability, about 127 mAh g^{-1} and 94.7 % capacity retention after 100 cycles even at 5.0 C rate.

Keywords Template-assisted method · Lithium iron phosphate · Cathode · Li-ion batteries

Introduction

Since the pioneering work of Padhi and coworkers [1] in 1997, the olivine structure lithium iron phosphate (LiFePO$_4$) has been recognized as a promising cathode material for lithium-ion batteries. Compared with other cathode materials, LiFePO$_4$ exhibits the advantages of high theory capacity (~170 mAh g^{-1}), excellent thermal stability, no toxicity, low cost, and high reversibility, and so on. However, its intrinsic low electronic conductivity (~10^{-9} S cm^{-1}) and low Li-ions diffusion coefficient (~10^{-14} cm^2 s^{-1}) limit the rate capability and then its application. Many efforts have been tried to solve these problems, such as coating some conductive materials on the surface of the particles, doping some cations or anions into the structure, and minimizing the particle size, etc. [2–6].

LiFePO$_4$ usually be prepared by using sol–gel, hydrothermal route, carbon thermal reduction, and rheological method [7–11], and some groups also have been synthesized by using various morphology cathode materials through a template-assisted method, and some very interesting results are obtained [12–14].

Cotton fiber, a kind of natural fiber, is mainly composed of cellulose. The cotton fiber is very suitable for template because it, without having being removed after chemistry reaction, is very cheap and environmentally friendly. In fact, cotton fiber has been used as a template to synthesize metal oxide microtubules such as biomorphic SnO$_2$ microtubules [15] and TiO$_2$ hollow fibers [16]. Therefore, the cheap cotton fiber was chosen as the template to synthesize the carbon microtubules core structure LiFePO$_4$ in the experiment. The structure, morphology, and electrochemical performances are studied in detail.

T. Wumair · J. Dou · L. Zhang · M. Chen · X. Kang
Xinjiang Technical Institute of Physics and Chemistry,
Chinese Academy of Sciences, Urumqi Xinjiang 830011, China

J. Dou · L. Zhang · M. Chen
Graduate University of Chinese Academy of Sciences,
Beijing 100049, China

T. Wumair (✉) · J. Dou · L. Zhang · M. Chen · X. Kang
Xinjiang Key Laboratories of Electronic Information
Materials and Devices, Urumqi Xinjiang 830011, China
e-mail: turdi@ms.xjb.ac.cn

Experiments

Preparation of the carbon microtubules core structure LiFePO$_4$

The carbon microtubules core structure LiFePO$_4$ was synthesized by using a template-assisted method (cotton fiber as the template). All the reagents used in the experiment were in analytical purity and used without further purification.

FePO$_4$·2H$_2$O and Li$_2$CO$_3$ were chosen as starting materials to prepare the precursor and oxalic acid as both complexant and reductant. The stoichiometric amount of FePO$_4$·2H$_2$O, Li$_2$CO$_3$, and oxalic acid were dissolved in an appropriate quantity of distilled water with continuous stirring at 90 °C, until a light green clear sol was obtained. Then, an appropriate amount of cotton fiber was added into the green sol and stirred continually at 90 °C for 10 h. After washing and filtering, the precursor was sintered at 350 °C for 5 h and at 700 °C for 10 h, respectively, under N$_2$ atmosphere to prevent the formation of Fe^{3+} impurities.

For comparison, we also prepared LiFePO$_4$/C using a conventional sol–gel method with the same reagents used above, and the sintering process was also the same as above.

To evaluate the carbon content in the prepared composites, a simple method was used as described in articles [17, 18]. The sample was heated to 700 °C at a rate of 5 °C/min for 6 h in air to burn off the residual carbon. At the same time, the LiFePO$_4$ will be oxidized to Li$_3$Fe$_2$(PO$_4$)$_3$ and Fe$_2$O$_3$ (the weight will be increased by 5.1 %). So, the amount of carbon content can be calculated as follows:

$$c = (m-m')\big/m + 0.051 \qquad (1)$$

where c is the carbon content, and m and m' are the weight of the sample before and after heat treatment. Based on Eq. (1), we can calculate the carbon content of the prepared carbon microtubules core structure LiFePO$_4$ to be about 13.2 %.

Characterization of the carbon microtubules core structure LiFePO$_4$

The crystalline phase was analyzed by X-ray diffraction (XRD, RINT-2500V, Rigaku Co.) with Cu Kα radiation (λ=1.5418 Å) in the range of $15°\leq2\theta\leq75°$ with a scanning rate of 2° per min. The particle morphologies of the prepared powders were determined by field emission scanning electron microscopy (FESEM, Supra 55VP).

Cell assembly and electrochemical tests

Electrochemical performances of the prepared LiFePO$_4$ were investigated using CR2025 coin cell. The cathode was fabricated from a mixture of the as-synthesized powders, acetylene black, and polyvinylidene fluoride with a weight ratio of 80:15:5, and the electrolyte was 1 M LiPF$_6$ in a mixture of ethyl carbonate, diethyl carbonate, and dimethyl carbonate (volume ratio 1:1:1). The slurry was then cast on an aluminum foil and dried at 120 °C overnight under a vacuum. The cells (CR2025) were assembled in an argon-filled glove box using a lithium metal foil as the counter electrode and microporous polypropylene sheet

(Celgard 2400, Celgard, Inc., USA) as the separator. The cells were charged and discharged between 2.3 and 4.3 V on a charge/discharge apparatus (BTS-51, Neware, China). Cyclic voltammetry (CV) and electrochemical impedance spectroscopy (EIS) were conducted by using the CHI650 electrochemical working station.

Results and discussion

Material characterizations

Figure 1 shows the XRD pattern of the carbon microtubules core structure LiFePO$_4$ (sample) which was prepared by using a template-assisted method. The strong and narrow diffraction peaks of the sample indicate that the orthorhombic olivine structure LiFePO$_4$ (JCPDS 83–2092) is successfully synthesized [19] in the experiment. All the diffraction peaks can be indexed on the basis of the orthorhombic olivine-type structure with the *Pnma* space group. In addition, there are no any other peaks such as carbon diffraction peaks found, indicating that the cotton fiber did not destroy the lattice of LiFePO$_4$, and the generated carbon may exist in an amorphous state.

Since the morphology and particle sizes of LiFePO$_4$ have a great influence on their electrochemical performance, FESEM and TEM analyses of the prepared carbon microtubules core structure LiFePO$_4$ were carried out. The FESEM and TEM images are shown in Fig. 2. A carbon microtubules core structure is clearly shown in Fig. 2a, b. The diameter of the carbon microtubule is about 6 μm, the wall thickness is about 0.8 μm, and the LiFePO$_4$ particles (about 50~100 nm) are distributed on the surface of the carbon microtubules. Such a structure is favorable for Li$^+$ ions diffusion and electrons transport during the charge and discharge process. Because the electrolyte is able to penetrate into the carbon
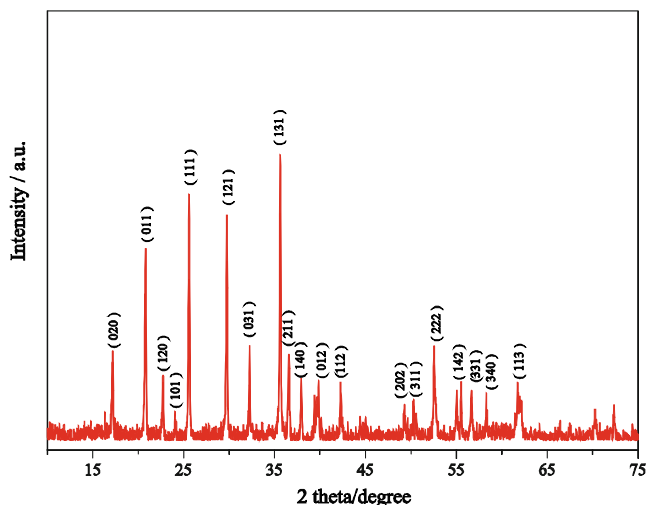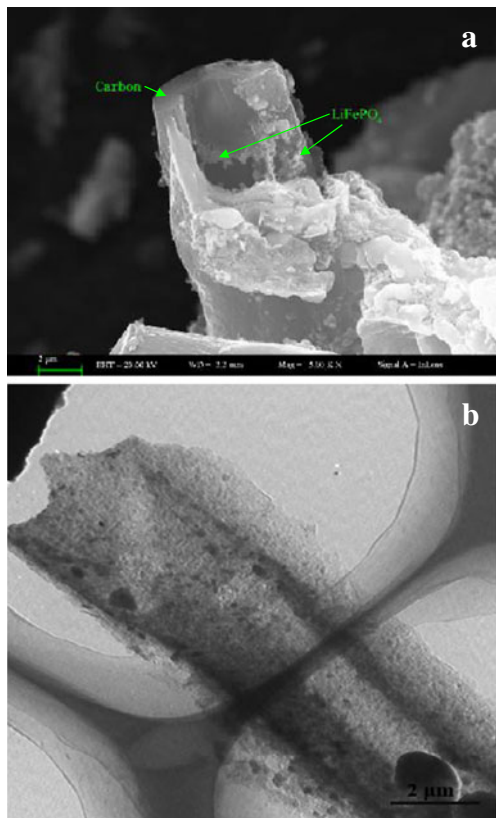

Fig. 1 XRD patterns of the LiFePO$_4$

Fig. 2 FESEM and TEM images of as-synthesized LiFePO$_4$

microtubules, reduce the diffusion distance of Li$^+$ ions, and increase the contact area between cathode material and electrolyte, these are all the benefits for Li$^+$ ions diffusion. At the same time, the carbon microtubules can provide a channel for electrons transport, decreasing the cell resistance and improving the electron conductivity of the cathode material, as shown in Fig. 3. The electrons will transport along the wall of the carbon microtubules easily, and the Li$^+$ ions will migrate directly into the electrolyte in charge process.
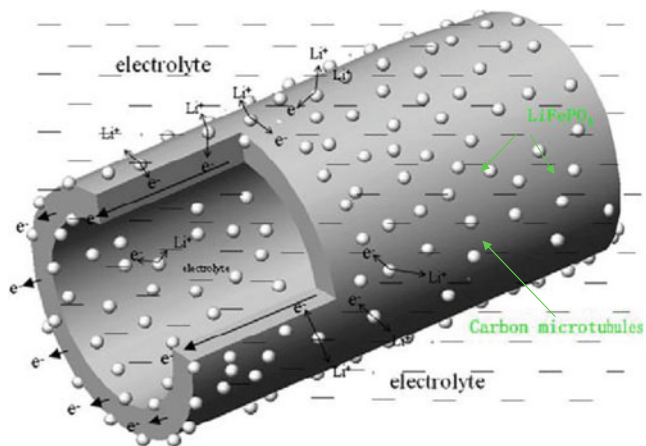

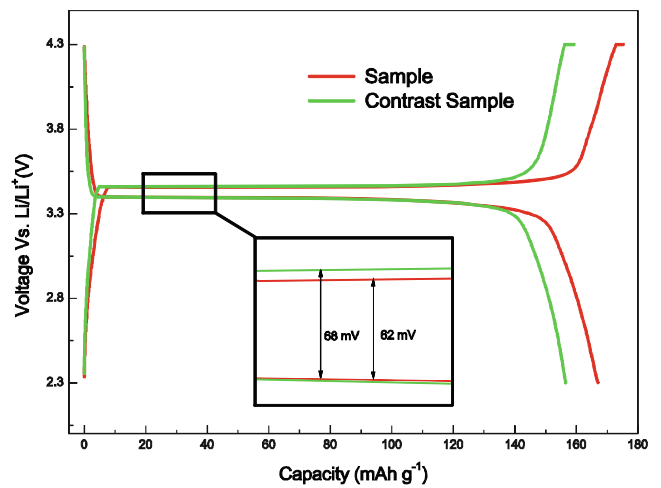Fig. 3 The conductive mechanisms diagram of the as-synthesized LiFePO$_4$ in charge process

Fig. 4 The initial charge/discharge curves of the as-synthesized LiFePO$_4$ and the contrast sample LiFePO$_4$

Electrochemical properties

The initial charge–discharge curves of the as-synthesized LiFePO$_4$ and the contrast sample between 2.3 and 4.3 V at 0.2 C (1.0 C=150 mA/g) rate are shown in Fig. 4 (the obtained charge or discharge capacity is calculated based on LiFePO$_4$ not including the amorphous carbon). The two samples are all shown as a long and flat voltage plateau at 3.397~3.459 and 3.396~3.464 V (according to the initial discharge capacity of 167 and 156 mAh g^{-1}, respectively), which is the main characteristic of the two-phase reaction of LiFePO$_4$. The polarization potential of the as-synthesized samples and contrast sample is 62 and 68 mV, respectively (insert of Fig. 4), indicating that the kinetics of the as-synthesized samples is indeed improved. Especially, the polarization potential of the as-synthesized samples is only 62 mV, which is smaller than the previous reports [20, 21],
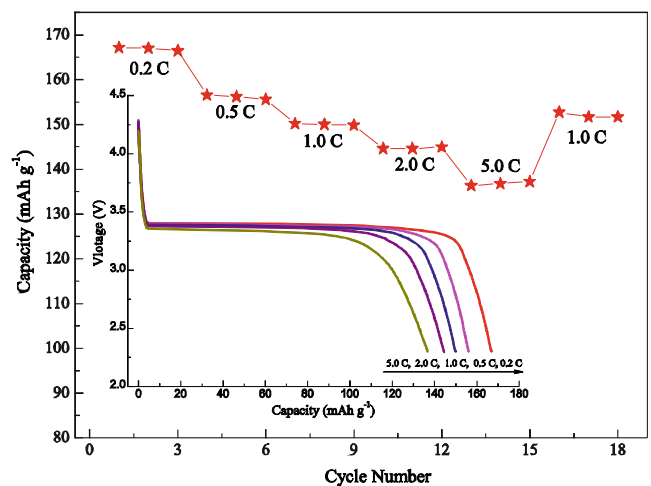

Fig. 5 The discharge curves and the rate performance of the as-synthesized LiFePO$_4$ at 0.2, 0.5, 1.0, 2.0, and 5.0 C rate under room temperature
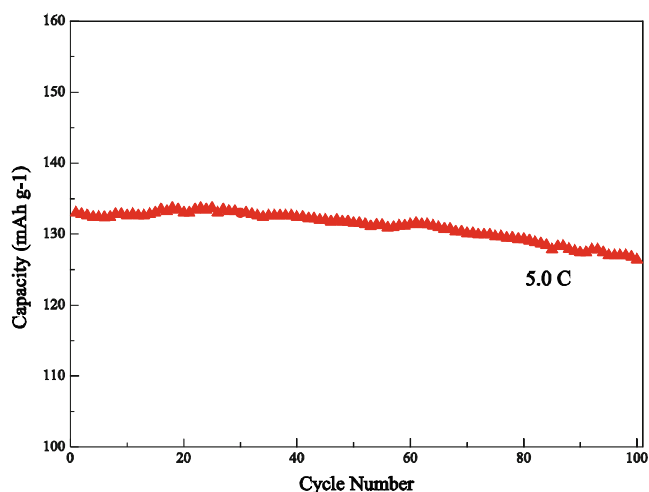
Fig. 6 The cycling curves at 5.0 C rate under room temperature

indicating a higher reaction kinetics of the as-synthesized LiFePO$_4$ and better electrochemical reversibility.

Figure 5 shows the discharge curves and the rate performance of the as-synthesized LiFePO$_4$ at 0.2, 0.5, 1.0, 2.0, and 5.0 C rate under room temperature. It was seen that with the current density increasing gradually, the discharge capacity of the LiFePO$_4$ also decreases. The discharge capacities are 167, 156, 150, 144, and 136 mAh g^{-1} at 0.2, 0.5, 1.0, 2.0, and 5.0 C rate, respectively. At the same time, when recovering the former testing rate (1.0 C rate in the experiment), the discharge capacity which almost has no any decrease indicates the good cyclic reversibility of the electrode. In addition, as the discharge current increases, the discharge capacity gradually decreases, but the electrode still maintains a long and flat voltage plateau as shown in Fig. 5. This phenomenon is directly related to the short Li$^+$ ions diffusion distance and high electrons conductivity during charge–discharge progress and then the good cyclic reversibility.
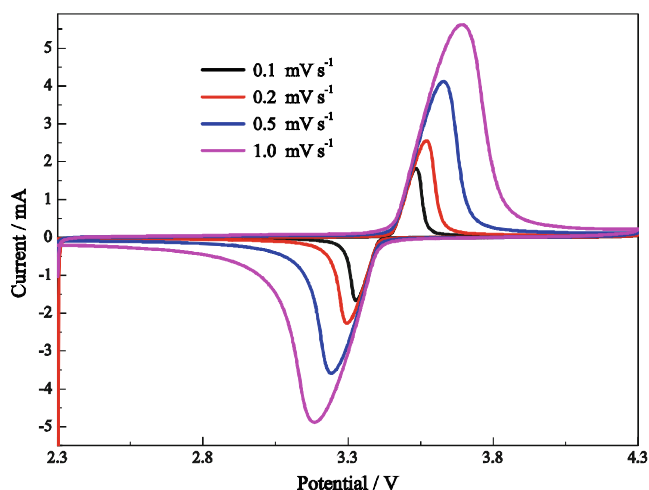

Fig. 7 The CV profiles of the as-synthesized LiFePO$_4$ electrode between 2.3 and 4.3 V at different scanning rates (0.1, 0.2, 0.5, and 1.0 mV s^{-1})
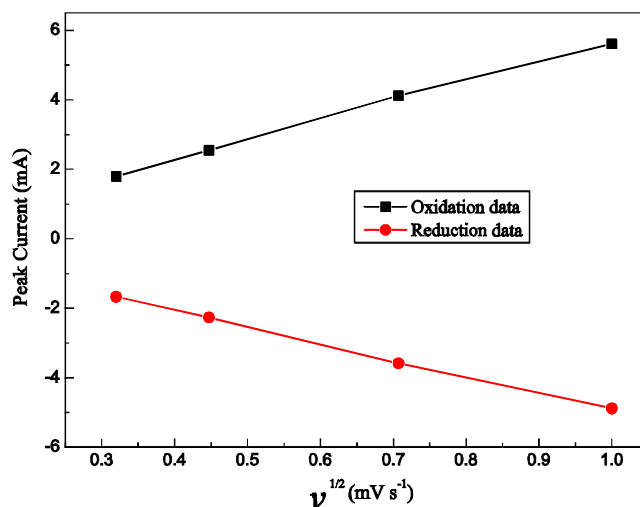

Fig. 8 Variation of redox peak current I_p to scan rate $v^{1/2}$ for the as-synthesized LiFePO$_4$ material

In addition, the cycle performance of the as-synthesized sample was also measured. The cycling curves at 5.0 C rate under room temperature are shown in Fig. 6. The discharge capacities are 127 mAh g^{-1} after 100 cycles. The discharge capacity retentions are about 94.7 %. It shows good cycling stability, and the electrode shows only a capacity fading of 0.05 % per cycle. It is also attributed to the short Li$^+$ ions diffusion distance and high electrons conductivity in the carbon microtubules core structure LiFePO$_4$, and then the low irreversible capacity loss, to good cycling stability even at a high rate.

CV measurements

CV is a well-suited technique to evaluate the cathode performance and electrode kinetics. Figure 7 shows the CV profiles of the as-synthesized LiFePO$_4$ electrode between 2.3 and 4.3 V at different scanning rates (0.1, 0.2, 0.5, and
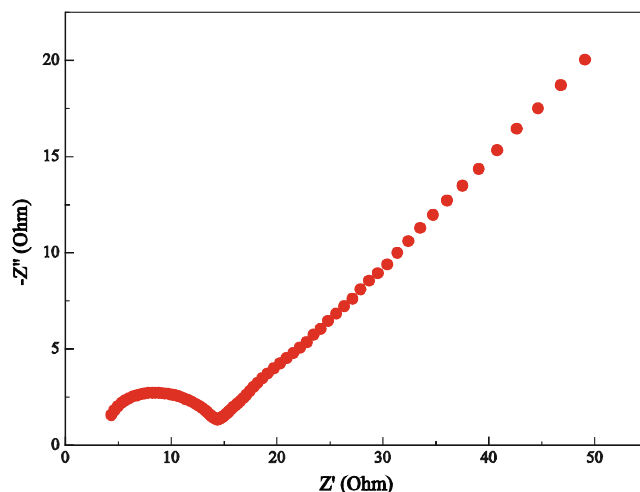

Fig. 9 The Nyquist plot of the as-synthesized LiFePO$_4$ tested at fully discharged state (2.3 V)

1.0 mV s^{-1}, respectively). A couple of redox peaks is observed at 3.328 and 3.535 V in the CV curve obtained at the scanning rate of 0.1 mV s^{-1}. These peaks correspond to the extraction and insertion of lithium ions in the electrode. As the scanning rate is raised, the oxidation peak current shifts to a higher and the reduction peak current shifts to lower, indicating the increased kinetic polarization and increased internal resistance [22]. Because the peak current I_p is proportional to the square root of the scan rate $v^{1/2}$ (as shown in Fig. 8), so I_p can be expressed by the classical Randles–Sevchik equation:

$$I_p = 2.69 \times 10^5 n^{3/2} A D^{1/2} C v^{1/2} \qquad (2)$$

where n is the number of electrons per species reaction, A is the interface between the electrolyte and the active material, C is the concentration of Li$^+$ ions, D is the diffusion coefficient of Li$^+$ ions, and v is the potential scan rate. Based on Eq. (2) and the scan rate, peak current, the apparent diffusion coefficient of Li$^+$ ions can be calculated to be at an order of 10^{-11} cm^2 S^{-1} for both charging and discharging electrodes. The obtained Li$^+$ ions diffusion coefficient by CV curves is three orders of magnitude larger than the pure LiFePO$_4$ (~10^{-14} cm^2 S^{-1}). However, the value of lithium-ion diffusion coefficient D obtained by CV is not accurate enough in such a two-phase reaction system, and the value of D may be overestimated, because the liquid electrolyte could penetrate into the carbon microtubules core structure LiFePO$_4$ during charge and discharge process [23–25] as discussed above.

EIS measurements

To further understand the kinetics process of the electrode materials, EIS measurements were carried out in the two-electrode coin cell CR2025. The Nyquist plot of the as-synthesized LiFePO$_4$ sample was presented in Fig. 9. The semicircle at high-to-medium frequency is attributed to the charge transfer resistance (R_{ct}), and the inclined line at low frequency represents Li$^+$ ions diffusion resistance in electrode bulk, namely, the Warburg impedance. The numerical value of diameter of the semicircle (at high-to-medium frequency) on the real axis is approximately equal to R_{ct} [26]. As shown in Fig. 9, the as-synthesized LiFePO$_4$ electrode exhibits the R_{ct} as small as about 15 Ω, indicating the low electrochemical polarization, fast electrode/electrolyte interface reaction, and lithium diffusion processes. The low electrochemical resistances are attributed to the special structure of the as-synthesized LiFePO$_4$ material, which is favorable for Li$^+$ ions diffusion and electrons transport.

Conclusion

The carbon microtubules core structure LiFePO$_4$ was synthesized by using a cotton fiber template-assisted method. XRD and FESEM analysis indicate that the well-crystallized carbon microtubules core structure LiFePO$_4$ was successfully prepared. The charge–discharge tests show that the prepared composite has good electrochemical performances as follows:

1. High discharge capacity (the initial discharge capacity is 167 mAh g^{-1} at 0.2 C rate)
2. Good rate performance (167, 156, 150, 144, and 136 mAh g^{-1} at 0.2, 0.5, 1.0, 2.0, and 5.0 C rate, respectively)
3. Good high rate cycling stability (retained about 94.7 % of its initial capacity after 100 cycles even at 5.0 C rate)

These performances attribute to the special structure, which is favorable for Li$^+$ ions diffusion (shortening the diffusion distance of Li+ions) and electrons transport (providing the channel for electrons transport). The results demonstrated that a cotton fiber template-assisted method is a promising approach to prepare high-performance LiFePO$_4$ composite for lithium-ion batteries.

References

1. Padhi AK, Nanjundaswamy KS, Goodenough JB (1997) J Electrochem Soc 144:1188–1194
2. Shin HC, Nam KW, Chang WY (2011) Electrochim Acta 56:1182–1189
3. Zhang W, Hu Y, Tao X, Huang H, Gan YP, Wang CT (2010) J Phys Chem Solids 71:1196–1200
4. Zhang Q, Wang SM, Zhou ZF, Ma GL, Jiang WW, Guo XS, Zhao S (2011) Solid State Ionics 191:40–44
5. Liu H, Feng Y, Wang Z, Wang K, Xie JG (2008) Powder Technol 184:313–317
6. Zhao L, Hu YS, Li H, Wang ZX, Chen LQ (2011) Adv Mater 23:1385–1388
7. Liu YY, Cao CB, Li J (2010) Electrochim Acta 55:3921–3926
8. Gaberscek M, Dominko R, Bele M, Remskar M, Hanzel D, Jamnik J (2005) Solid State Ionics 176:1801–1805
9. Liang GC, Wang L, Ou X, Zhao X, Xu SZ (2008) J Power Sources 184:538–542
10. Wang LN, Zhang ZG, Zhang KL (2007) J Power Sources 167:200–205
11. Zhong M, Zhou ZT (2010) Solid State Ionics 181:1607–1610
12. Liu XH, Wang JQ, Zhang JY, Yang SR (2006) Chin J Chem Phys 19:530–534

13. Sides CR, Croce F, Young VY, Martin CR, Scrosati B (2005) Electrochem Solid-State Lett 8:A484–A487
14. Yang ST, Yue HY, Yin YH, Yang JX, Yang WG (2006) Electrochim Acta 51:4971–4976
15. Sun B, Fan TX, Xu JQ, Zhang D (2005) Mater Lett 59:2325–2328
16. Su BT, Wang K, Hu CL, Mu HM, Dong N, Tong YC, Bai J (2008) Chem Regents 30:112–114
17. Beninati S, Damen L, Mastragostino M (2008) J Power Sources 180:875–879
18. Belharouak I, Johnson C, Amine K (2005) Electrochem Commun 7:983–988
19. Yao JW, Wu F, Qiu XP, Li N, Su YF (2011) Electrochim Acta 56:5587–5592
20. Ge YC, Yan XD, Liu J, Zhang XF, Wang JW, He XG, Wang RS, Xie HM (2010) Electrochim Acta 55:5886–5890
21. Wang XC, Huang YD, Jia DZ, Guo ZP, Miao M (2012) Preparation and characterization of high-rate and long-cycle LiFePO$_4$/C nanocomposite as cathode material for lithium-ion battery. J Solid State Chem 16(1):17–24. doi:10.1007/s10008-010-1269-4
22. Lee KL, Jung JY, Lee SW, Moon HS, Park JW (2004) J Power Sources 130:241–246
23. Fey GTK, Huang KP, Kao HM, Li WH (2011) J Power Sources 196:2810–2818
24. Xie J, Imanishi N, Zhang T, Hirano A, Takeda Y, Yamamoto O (2009) Electrochim Acta 54:4631–4637
25. Tang K, Yu XQ, Sun JP, Li H, Huang XJ (2011) Electrochim Acta 56:4869–4875
26. Lu F, Zhou YC, Liu J, Pan Y (2011) Electrochim Acta 56:8833–8838